Electronic Supplementary Material (ESI) for Physical Chemistry Chemical Physics.

Supporting materials for

Selective excitation of hydrogen doubles the yield and improves the robustness of parahydrogen-induced polarization of low-γ nuclei

Andreas B. Schmidt,[1,2,3‡]* Arne Brahms,[4‡] Frowin Ellermann,[3] Stephan Knecht,[5] Jürgen Hennig,[1] Dominik von Elverfeldt,[1] Rainer Herges,[4] Jan-Bernd Hövener,[3] Andrey N. Pravdivtsev[3]*

1 Department of Radiology, Medical Physics, Medical Center, University of Freiburg, Faculty of Medicine, University of Freiburg, Killianstr. 5a, Freiburg 79106, Germany.

2 German Cancer Consortium (DKTK), partner site Freiburg and German Cancer Research Center (DKFZ), Im Neuenheimer Feld 280, Heidelberg 69120, Germany.

3. Section Biomedical Imaging, Molecular Imaging North Competence Center (MOIN CC), Department of Radiology and Neuroradiology, University Medical Center Kiel, Kiel University, Am Botanischen Garten 14, 24118, Kiel, Germany.

4. Otto Diels Institute for Organic Chemistry, Kiel University, Otto-Hahn-Platz 5, 24118, Kiel, Germany.

5 NVision Imagning Technologies GmbH, 89081 Ulm, Germany

KEYWORDS. Parahydrogen, MR signal enhancement, hyperpolarization, INEPT, spin order transfer, polarization transfer, ethyl pyruvate, ethyl acetate, 2-hydroxyethyl propionate

Contents

1. Chemicals 3
2. pH_2 polarization setup 5
3. Schematics of SEPP-INEPT+ and ESOTHERIC pulse sequences 6
4. phSPINEPT+ polarization transfer 7
   - 4.1. Polarization transfer results 7
   - 4.2. Polarization transfer maps (Simulations) 8
     - A. Methods 8
     - B. 1-^{13}C-Vinyl acetate to 1-^{13}C-ethyl acetate 8
     - C. 1-^{13}C-Vinyl acetate-d_6 to 1-^{13}C-ethyl acetate-d_6 9
     - D. 1-^{13}C-Vinyl pyruvate to 1-^{13}C-ethyl pyruvate 10
     - E. 1-^{13}C-Vinyl pyruvate-d_6 to 1-^{13}C-ethyl pyruvate-d_6 12
     - F. 1-^{13}C- Hydroxyethyl acrylate-d^8 to 1-^{13}C- Hydroxyethyl propionate-d_8 14
     - G. 1-^{13}C- Hydroxyethyl acrylate-d_3 to 1-^{13}C- Hydroxyethyl propionate-d_3 16
     - H. Efficiency of phSPINEPT+ in various three spin systems 17
   - 4.3. phINEPT+ and phSPINEPT+ spectra (Experimental) 18
     - A. 1-^{13}C-Vinyl acetate to 1-^{13}C-ethyl acetate 18
     - B. 1-^{13}C-Vinyl acetate-d_6 to 1-^{13}C-ethyl acetate-d_6 19
     - C. 1-^{13}C-Vinyl pyruvate to 1-^{13}C-ethyl pyruvate 20
     - D. 1-^{13}C-hydroxyethyl acrylate-d_3 to 1-^{13}C-hydroxyethyl propionate-d_3 21
5. Estimation of hydrogenation reaction and magnetization decay 23
6. Scripts: pulse sequences (Bruker code) 25
   - A. SOT frame 25
   - B. SOT: phINEPT+ 25
   - C. SOT: phSPINEPT+ 25
   - D. SOT: phSPINEPT+^{001} 25
   - E. phSPINEPT+^{010} 25
   - F. phSPINEPT+^{011} 26
7. References 27

1. Chemicals

The following compounds were used without any additional purification: the substrate precursors hydroxyethyl acrylate-1-^{13}C,2,3,3-d$_3$ (HEA-d$_3$, CAS 1216933-17-3, Sigma Aldrich, USA), vinyl acetate (VA, CAS 108-05-4, Sigma Aldrich, USA), vinyl acetate-d$_6$ (VA-d6, CAS 189765-98-8, CDN isotopes, CA; distributed by EQ Laboratories GmbH, DE); the solvents chloroform-d (CAS 865-49-6, Sigma Aldrich, USA) and acetone-d$_6$ (CAS 666-52-4, Deutero GMBH, DE); and the hydrogenation catalyst [1,4-Bis-(diphenylphosphino)-butan]-(1,5-cyclooctadien)-rhodium(I)-tetrafluoroborat ([Rh], CAS 79255-71-3, Sigma Aldrich, USA). The substrate precursor vinyl pyruvate (VP, 80%) was synthesized in house; the protocol and quality assurance will be published elsewhere. The concentrations of the precursors and catalyst used in experiments are reported in **Tab S1** together with the achieved polarization values.

In the hyperpolarization experiments, VA and VA-d$_6$ were hydrogenated into ethyl acetate (EA) and ethylacetate-d$_6$ (EA-d$_6$), respectively; VP was reacted into ethyl pyruvate (EP); HEA-d$_3$ formed hydroxyethyl propionate-d$_3$ (HEP-d$_3$).

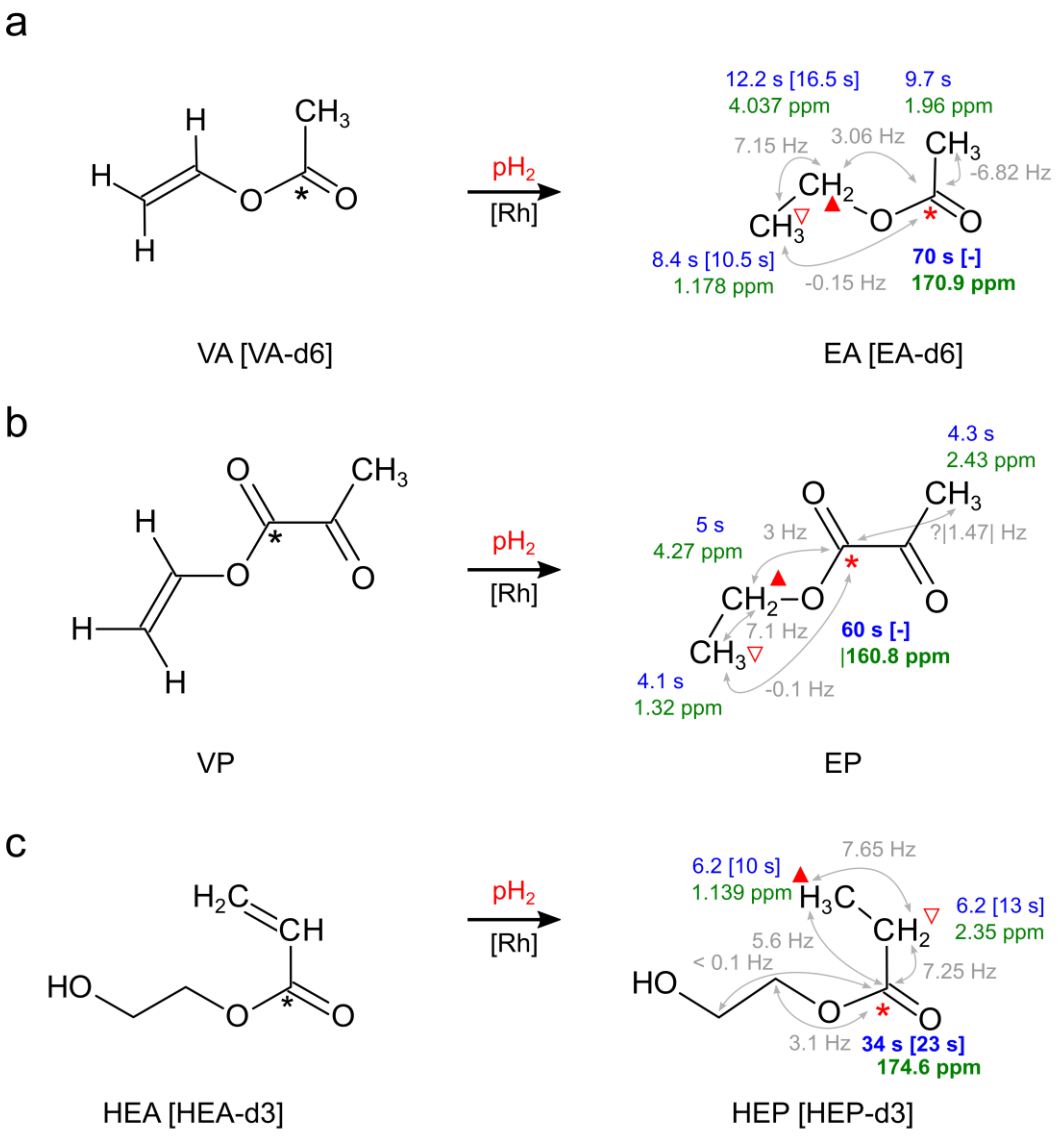

Figure S1. Chemical structure and hydrogenation reactions of VA→EA, VP→EP, HEA→HEP. T1 relaxation times, J-coupling constants, and chemical shifts of the relevant proton and carbon-13 sites are shown (blue, gray, and green, respectively). The J-coupling constants and chemical shifts were used to calculate polarization transfer in phINEPT+ and phSPINEPT+ experiments. Values in brackets corresponds to deuterated substrates. All T_1-values, chemical shifts and J-coupling constants were measured customly at 330 K in chloroform-d at 9.4 T (see **Fig S2**, fitted 1-^{13}C-HEP spectrum,). Only HEP-d3 ^{1}H T$_1$ values are reported for ^{13}C labeled molecules, all the rest were measured at natural abundance. The red solid and hollow triangles indicate the pH$_2$-nascent ^{1}H; the red asterisk indicates the ^{13}C site of interest towards which polarization was transfered in our experiments.

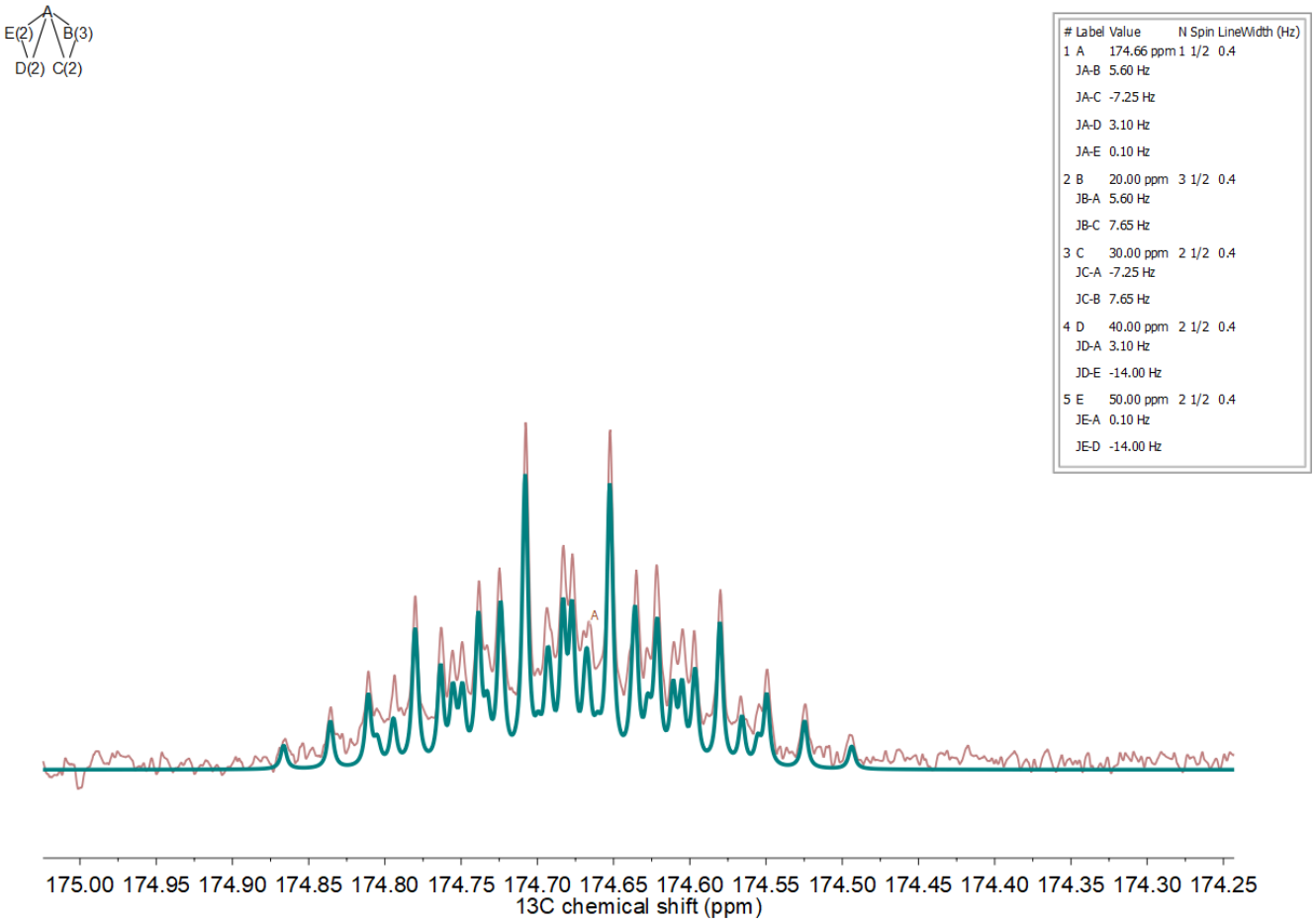

Figure S2. ^{13}C NMR spectrum of 1-^{13}C-HEP (red, natural abundance) in chloroform-d at 330 K and 9.4 T and fitted spectrum (green). The determined J-coupling constants are given in the insert table and in **Fig S1** and were used for the simulations.

2. pH_2 polarization setup

All experiments were carried out on a 400 MHz widebore nuclear magnetic resonance (NMR) system (WB NMR 400 MHz, Avance Neo, 9.4 T, Bruker, DE) using a 5 mm BBFO probe. A medium wall high-pressure 5 mm NMR tubes were used (524-PV-7, Wilmad-LabGlass, USA). The hyperpolarization setup (**Fig S3**) allowed flushing gaseous pH_2 through the samples at elevated pressure (7.8 bar). The stepwise experimental procedurewas as follows:

1. 450 µL of the catalyst-precursor containing sample were filled into the NMR tube..
2. Gas from the tubing that enters the liquid sample was replaced by purging N_2 for approximately 5s.
3. The NMR tube was connected to the gas system.
4. The NMR tube was positioned in the NMR spectrometer.
5. The temperature of the probe and sample were equilibrated (about 2-3 minutes, 330 K).
6. The homogeneity of the static magnetic field was optimized using an automated routine (Topshim, Topspin 4.0.9, Bruker, DE).
7. The pressure was build up in the system without flushing pH_2 through the sample (solenoid valves S3 and S4 were opened for 5 seconds).
8. Pressure was build up and equilibrated in the gas-inlet and -outlet path from the NMR tube (S2 and S3 open for 25 ms, subsequently all S1-S4 valves were simultaneously; the 25 ms delay procedure preventing gas from streaming into the solution)
9. pH_2 gas was guided through the solution (S1 and S2 open for 6 seconds).
10. Stop the gas flow by equilibrating the inlet and outlet pressure (S1-S4 open for 1-2 s).
11. Polarization transfer and signal detection was performed (S1-S4 were kept open; ^1H decoupling was turned on when ^{13}C signals were acquired).

Note that the steps 3-11 were automated and fully controlled via the pulse program and TTL outputs of the NMR system and a microcontroller-based power relais box.

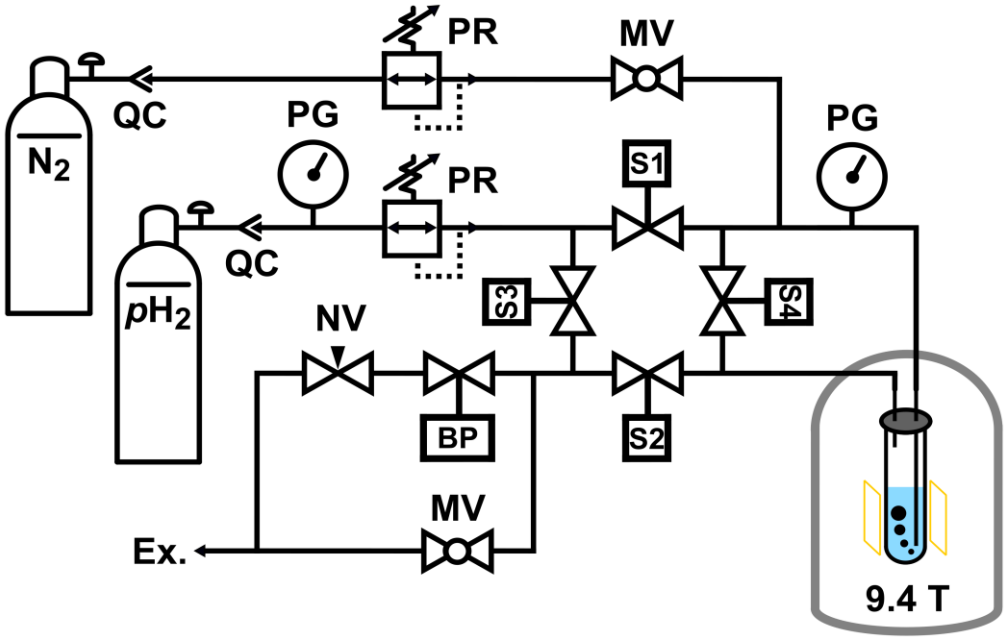

Figure S3. Scheme of the pH_2 bubbling system. The main components of the system are pressure gauges (PG), pressure regulators (PR), solenoid valves ([S]), quick connectors (QC), backpressure valve ([BP]), needle valves (NV), and manual shut-off valves (V). A part of the system can be flushed with N_2.

3. Schematics of SEPP-INEPT+ and ESOTHERIC pulse sequences

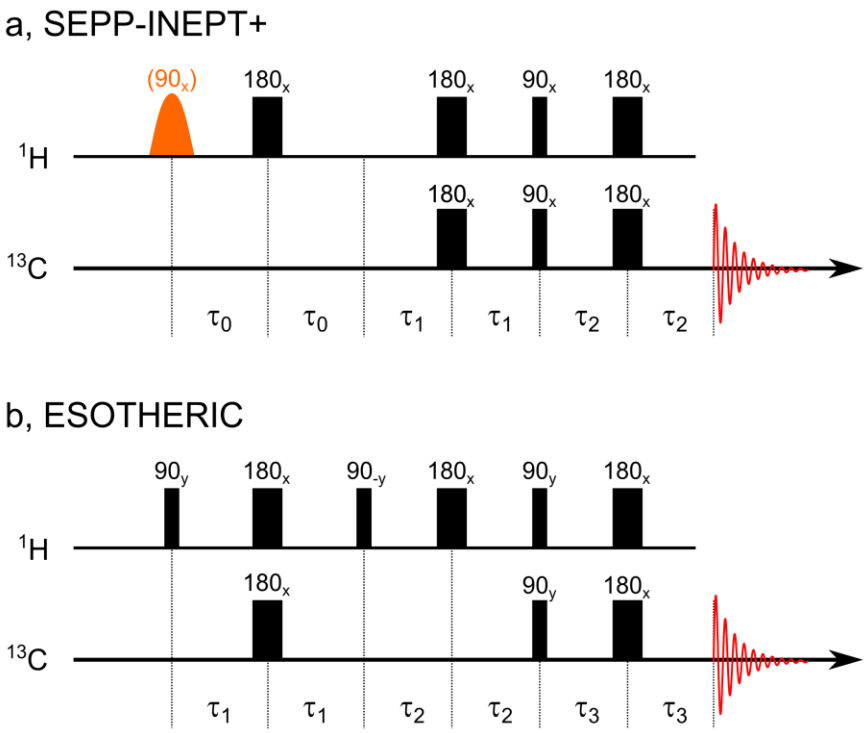

F

Figure S4. Schematics of the SEPP-INEPT+[2] (a) and ESOTHERIC[3] sequence (b). The sequences consist of non-selective radiofrequency hard pulses (black bars) with flip angle of 90° or 180° and phase x, y, -x, or -y on the ^{1}H and ^{13}C channel. SEPP-INEPT+ starts with a frequency selective ^{1}H pulse (orange).

4. phSPINEPT+ polarization transfer

4.1. Polarization transfer results

Table S1. Experimental parameters and polarization yield for each investigated substrate and sequence. $\boldsymbol{P^{th}}$ is the theoretical maximum ^{13}C-polarization at perfect conditions with 100% pH_2; $\boldsymbol{P^{exp}}$ is the experimentally observed ^{13}C-polarization with 50% pH_2 (values reported in the main text are indicated in **bold green**). If 100 % pH_2 would have been used (e.g. when produced with a helium cooled system[4]), the observed polarizations were 3 times larger. The same applies for the reported ^{1}H multiplet polarization values $\boldsymbol{P_m^{th}}$, $\boldsymbol{P_m^{exp}}$. The total hydrogenation time t_h corresponds to the sum of steps 9 and 10 in section 2. All experiments were conducted at 330 K, 7.8 bar pH_2 and 9.4 T. For HEP, some experiments were not performed (indicated with $\boldsymbol{P^{exp}} = -$), and the experimentally used parameters (τ^{exp}) were different from the optimal values predicted by our simulations (τ^{th}).

PHIP system	PASADENA	phINEPT+	phSPINEPT+	phSPI-NEPT+^{010}	phSPI-NEPT+^{001}	phSPI-NEPT+^{011}
VA-d6→EA-d6 in $CDCl_3$ c=1 mM (^{13}C n.a.) t_h = 8 s δ_{CDH} = 4.1 ppm	$P_m^{th} = 100$ % $P_m^{exp} = 21.9$ %	$\tau_1 = 103$ ms $\tau_2 = 78$ ms $P^{th} = 45$ % $\boldsymbol{P^{exp} = 5.7}$ **%**	$\tau_1 = 100$ ms $\tau_2 = 81$ ms $P^{th} = 90$% $\boldsymbol{P^{exp} = 12.8}$ **%**	$\tau_1 = 103$ ms $\tau_2 = 81$ ms $P^{th} = 90$ % $P^{exp} = 10.8$ %	$\tau_1 = 103$ ms $\tau_2 = 81$ ms $P^{th} = 90$ % $P^{exp} = 12.2$ %	$\tau_1 = 100$ ms $\tau_2 = 81$ ms $P^{th} = 90$ % $P^{exp} = 12.1$ %
1-^{13}C-HEA-d3→1-^{13}C-HEP-d3 **in acetone-d6, unless stated otherwise** c=1 mM (99 % ^{13}C) t_h = 8 s δ_{CDH} = 2.35 ppm δ_{CD2H} = 1.15 ppm	$P_m^{th} = 100$ % $P_m^{exp} = 19.8$ %	$\tau_1^{th} = 34$ ms $\tau_2^{th} = 19$ ms $P^{th} = 49.6$ % $\tau_1^{exp} = 34$ ms $\tau_2^{exp} = 17$ ms $P^{exp} = 4.8$ % **($\boldsymbol{P^{th}}$ = 42.5 %)** **in $CDCl_3$:** $\boldsymbol{P^{exp} = 6.4}$ **%**	s-CDH $\tau_1^{th} = 34$ ms $\tau_2^{th} = 172$ ms $P^{th} = 93.4$% $P^{exp} = -$	s-CDH $\tau_1^{th} = 34$ ms $\tau_2^{th} = 172$ ms $P^{th} = 93.4$ % $P^{exp} =$	s-CDH $\tau_1^{th} = 33$ ms $\tau_2^{th} = 34$ ms $P^{th} = 99.8$ % $\tau_1^{exp} = 36$ ms $\tau_2^{exp} = 44$ ms $P^{exp} = 10.0$ % ($P^{th} = 88$ %)	s-CDH $\tau_1^{th} = 33$ ms $\tau_2^{th} = 34$ ms $P^{th} = 99.8$ % $\tau_1^{exp} = 36$ ms $\tau_2^{exp} = 44$ ms $P^{exp} = 9.4$ % ($P^{th} = 88$ %)
			s-CD2H $\tau_1^{th} = 37$ ms $\tau_2^{th} = 141$ ms $P^{th} = 77.4$ % $\tau_1^{exp} = 34$ ms $\tau_2^{exp} = 98$ ms $P^{exp} = 0.3$ % ($P^{th} = 0.8$%)	s-CD2H $\tau_1 = 37$ ms $\tau_2 = 141$ ms $P^{th} = 77.2$ % $P^{exp} = -$	s-CD2H $\tau_1^{th} = 38$ ms $\tau_2^{th} = 45$ ms $P^{th} = 94.7$ % $\tau_1^{exp} = 34$ ms $\tau_2^{exp} = 36$ ms $P^{exp} = 9.6$ % ($P^{th} = 89$ %)	s-CD2H $\tau_1 = 38$ ms $\tau_2 = 45$ ms $P^{th} = 94.7$ % $\tau_1^{exp} = 34$ ms $\tau_2^{exp} = 36$ ms $P^{exp} = 9.9$ % **($\boldsymbol{P^{th}}$ = 89 %)** **in $CDCl_3$:** $\boldsymbol{P^{exp} = 15.8}$ **%**
VP→EP in $CDCl_3$ c=30 mM (^{13}C n.a.) t_h = 8 s δ_{CDH} = 4.33 ppm	$P_m^{th} = 100$ % $P_m^{exp} = 16$ %	$\tau_1 = 57$ ms $\tau_2 = 36$ ms $P^{th} = 7$ % $\boldsymbol{P^{exp} = 0.44}$ **%**	$\tau_1 = 57$ ms $\tau_2 = 34.5$ ms $P^{th} = 14$% $P^{exp} = 0.95$ %	$\tau_1 = 57$ ms $\tau_2 = 36$ ms $P^{th} = 13.9$ % $P^{exp} = 1.1$ %	$\tau_1 = 57$ ms $\tau_2 = 42$ ms $P^{th} = 16.9$ % $P^{exp} = 1.2$ %	$\tau_1 = 57$ ms $\tau_2 = 42$ ms $P^{th} = 16.9$ % $P^{exp} = 1.2$ %
						$\tau_1 = 57$ ms $\tau_2 = 36.5$ ms $P^{th} = 16.5$ % $\boldsymbol{P^{exp} = 1.3}$ **%**
VA→EA in $CDCl_3$ c=30 mM (^{13}C n.a.) t_h = 23 s – for INEPT and 8 s for PASADENA δ_{CDH} = 4.15 ppm	$P_m^{th} = 100$ % $\boldsymbol{P_m^{exp} = 17}$ **%**	$\tau_1 = 83$ ms $\tau_2 = 216$ ms $P^{th} = 7.7$% $\boldsymbol{P^{exp} = 0.10}$ **%**	$\tau_1 = 83$ ms $\tau_2 = 216$ ms $P^{th} = 15.5$ % $\boldsymbol{P^{exp} = 0.21}$ **%**	$\tau_1 = 85$ ms $\tau_2 = 216$ ms $P^{th} = 14.5$ % $\boldsymbol{P^{exp} = 0.24}$ **%**	$\tau_1 = 85$ ms $\tau_2 = 204$ ms $P^{th} = 16.5$ % $\boldsymbol{P^{exp} = 0.31}$ **%**	$\tau_1 = 85$ ms $\tau_2 = 204$ ms $P^{th} = 16.5$ % $\boldsymbol{P^{exp} = 0.24}$ **%**

4.2. Polarization transfer maps (Simulations)

A. Methods

To simulate the polarization transfer maps listed below, we used the MOIN-spin library[5]. All necessary J-coupling constants and chemical shifts are given in **Fig. S1.** RF pulses with infinitesimally small durations were used. No relaxation effect or magnetic field inhomogeneity were considered. 100% pH_2 was assumed. The initial state of the system was calculated at B_0 by removing all coherences in the Eigen basis of liquid state Hamiltonian of the system.

B. 1-^{13}C-Vinyl acetate to 1-^{13}C-ethyl acetate

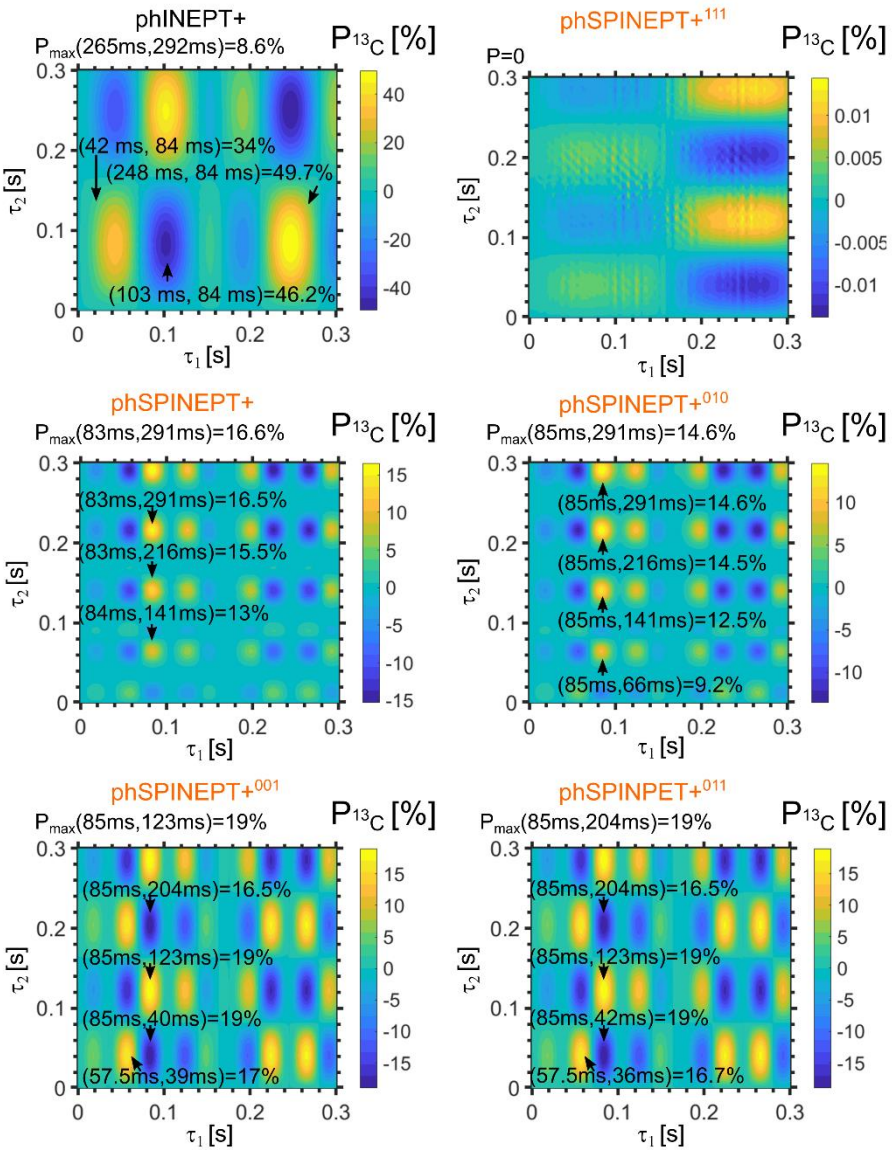

Figure S5. ^{13}C-polarization yield of 1-^{13}C-EA using phINEPT+ or phSPINEPT+ as a function of the two evolution time intervals τ_1 and τ_2. Eight protons (two stemming from pH_2) and one carbon at the acetate C1 position were considered (**Fig. S1**). The selective radio frequency pulses were set in resonance with the CH_2 protons of EA at the chemical shift of δ = 4.15 ppm.

C. 1-^{13}C-Vinyl acetate-d_6 to 1-^{13}C-ethyl acetate-d_6

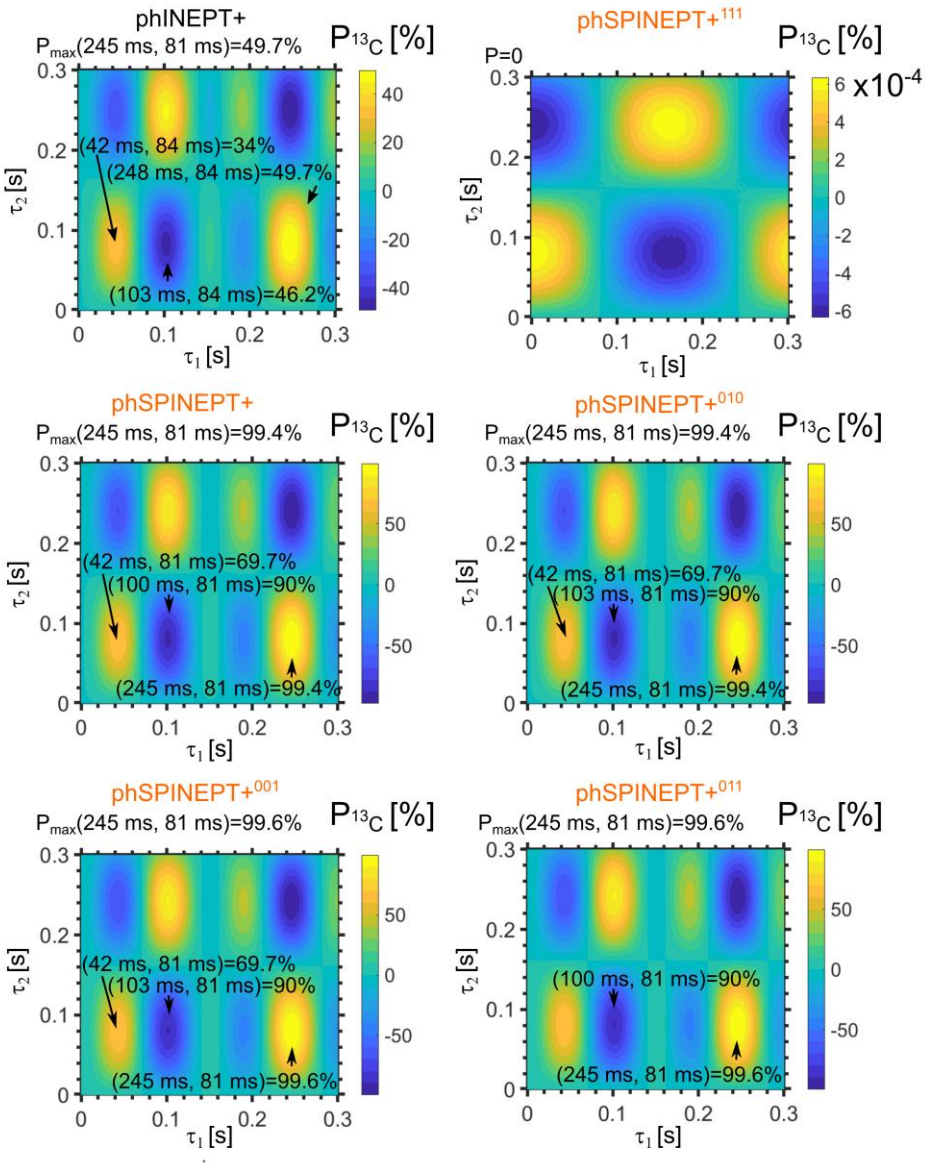

Figure S6. ^{13}C-polarization yield of 1-^{13}C-EA-d_6 using phINEPT+ or phSPINEPT+ as a function of the two evolution time intervals τ_1 and τ_2. Two protons (stemming from pH_2) and one carbon at the acetate C1 position were considered (**Fig. S1**). The selective radio frequency pulses were set in resonance with the CHD protons of EA-d_6 at the chemical shift of δ = 4.1 ppm.

D. 1-^{13}C-Vinyl pyruvate to 1-^{13}C-ethyl pyruvate

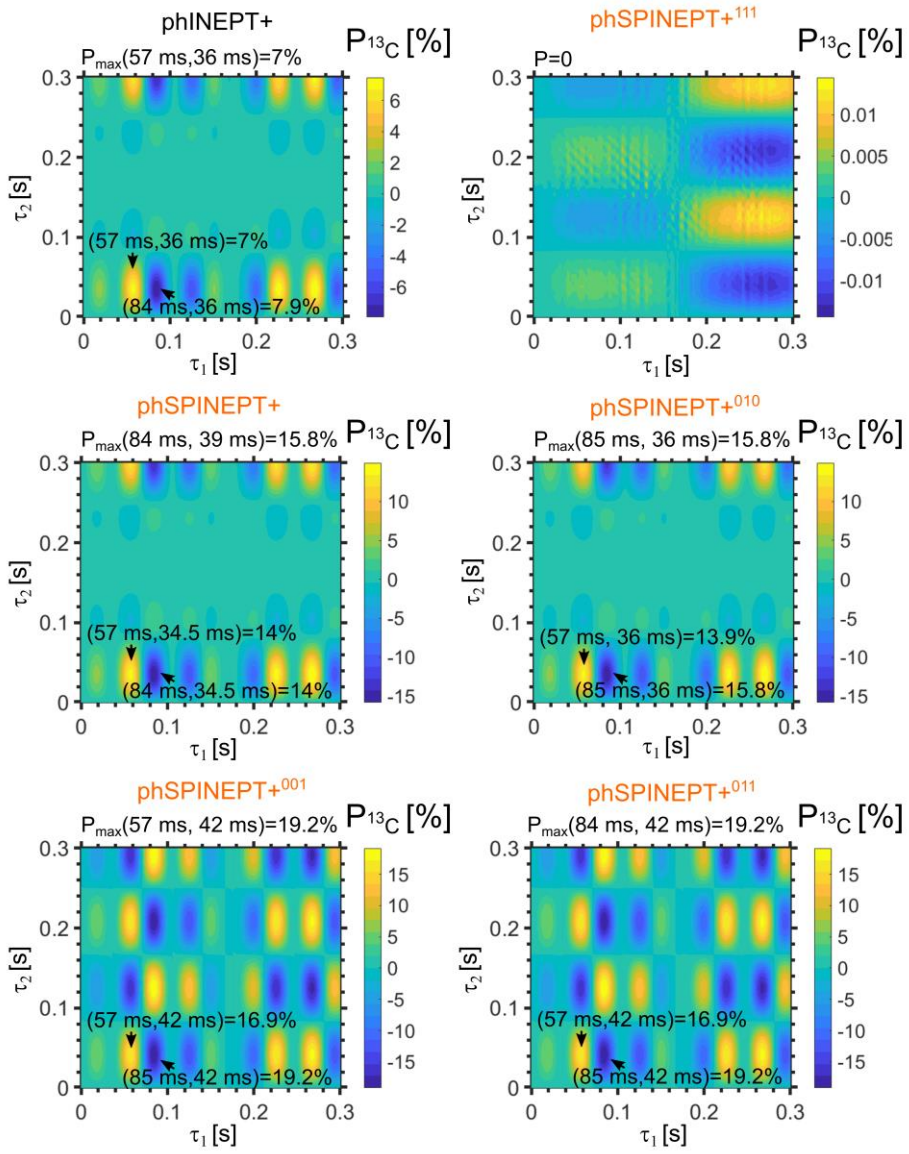

Figure S7. ^{13}C-polarization yield of 1-^{13}C-EP using phINEPT+ or phSPINEPT+ as a function of the two evolution time intervals τ_1 and τ_2. Eight protons (two stemming from pH2) and one carbon at the acetate C1 position were considered (**Fig. S1**). The selective radio frequency pulses were set in resonance with the CH_2 protons of EP at the chemical shift of δ = 4.33 ppm.

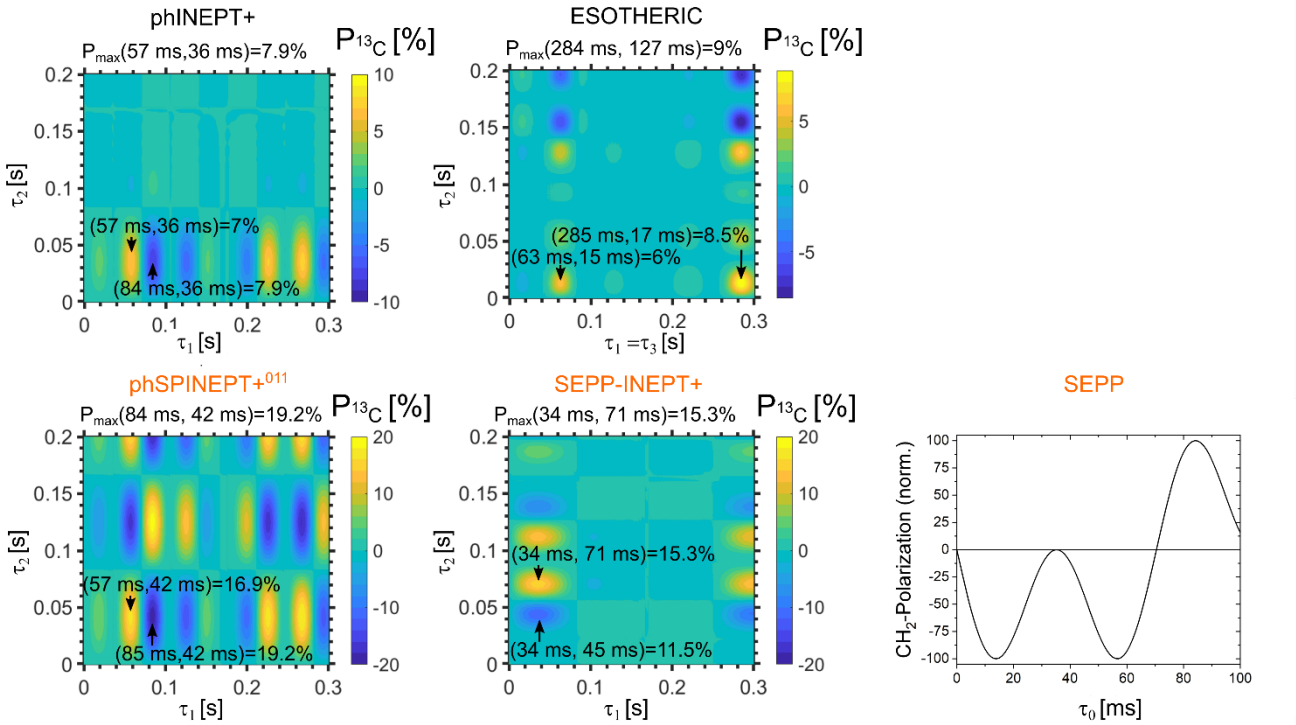

Figure S8. ^{13}C-polarization yield of 1-^{13}C-EP using phINEPT+, ESOTHERIC,[3] SEPP-INEPT+ and phSPINEPT+^{011} as a function of the two evolution time intervals $\boldsymbol{\tau_1}$ and $\boldsymbol{\tau_2}$. Eight protons (two stemming from pH_2) and one carbon at the acetate C1 position were considered (**Fig. S1**). The selective radio frequency pulses were set in resonance with the CH_2 protons of EP at the chemical shift of δ = 4.33 ppm. Note that there are 6 evolution intervals in ESOTHERIC (instead of four in phINEPT+) sequence, from which we kept $\boldsymbol{\tau_1 = \tau_3}$ as suggested by Korchak and coworkers; also, note that here $\boldsymbol{\tau}$-intervals are half of the **Δ**-intervals given in the ESOTHERIC scheme in the original work (see our Fig. S4).[3] The SEPP time interval $\boldsymbol{\tau_0}$ was optimized to give the maximum net polarization of the CH_2 protons (SEPP plot) after the SEPP block and was set to $\boldsymbol{\tau_0}$ ≅14 ms for SEPP-INEPT+. Note that this value deviates from $\frac{\mathbf{1}}{\mathbf{4}J_{HH}}$ ≅35 ms.

Table S2. Optimal SOT parameters τ_x, total time of SOT t_{total} and simulated polarization P^{th} under this conditions for 1-^{13}C-EP. Note that SEPP-INEPT is 16ms shorter than the phSPINEPT+^{011} but provides 4 % less polarization.

SOT sequence	$\boldsymbol{\tau_1}$ [ms]	$\boldsymbol{\tau_2}$ [ms]	$\boldsymbol{\tau_0}$ / $\boldsymbol{\tau_3}$ [ms]	$\boldsymbol{t_{total}}$ [ms]	$\boldsymbol{P^{th}}$ [%]
phINEPT+	84	36	-	240	8
phSPINEPT+^{011}	85	42	-	254	19.2
ESOTHERIC	285	17	285	1212	8.5
SEPP-INEPT+	34	71	14	238	15.3

E. 1-^{13}C-Vinyl pyruvate-d$_6$ to 1-^{13}C-ethyl pyruvate-d$_6$

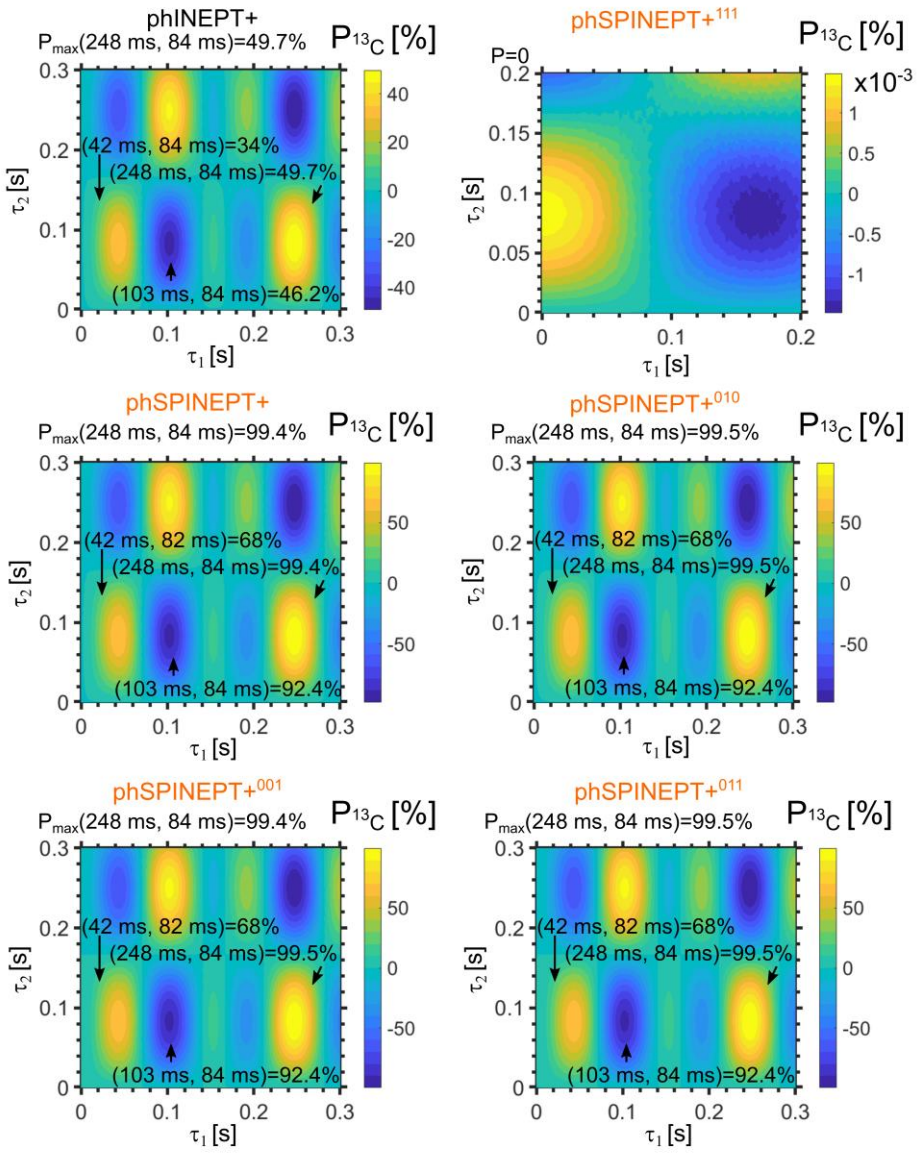

Figure S9. ^{13}C-polarization yield of 1-^{13}C-EP-d$_6$ using phINEPT+ or phSPINEPT+ as a function of the two evolution time intervals τ_1 and τ_2. Two protons (two stemming from pH_2) and one carbon at the acetate C1 position were considered (**Fig. S1**). The selective radio frequency pulses were set in resonance with the CHD protons of EP-d$_6$ at the chemical shift of δ = 4.33 ppm.

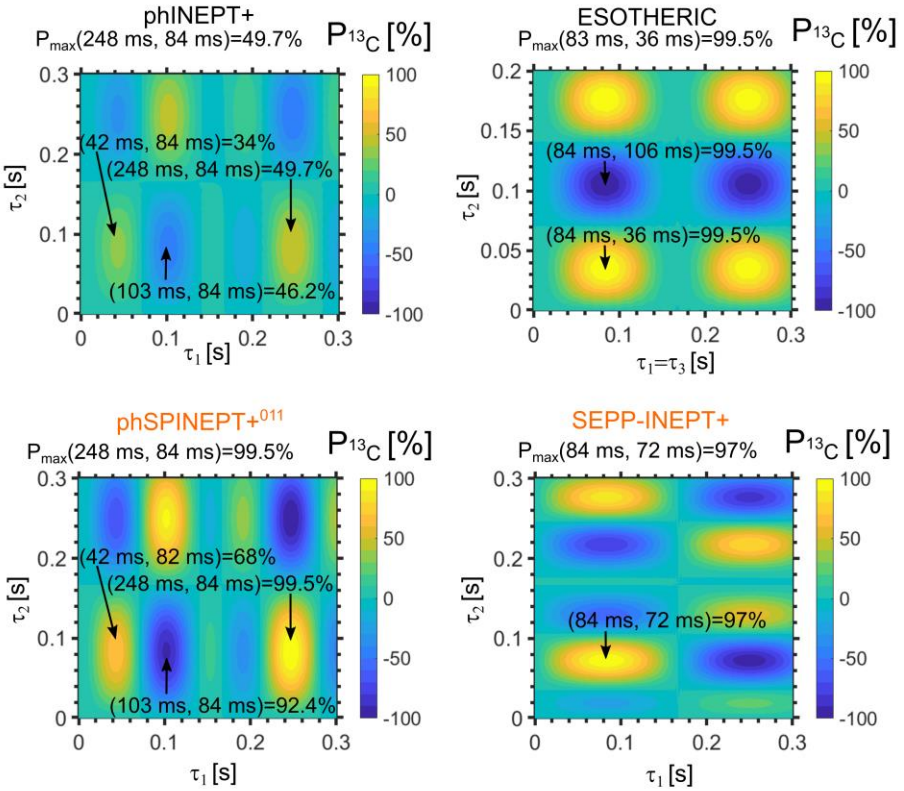

Figure S10. ^{13}C-polarization yield of 1-^{13}C-EP-d$_6$ phINEPT+, ESOTHERIC,[3] SEPP-INEPT+ and phSPINEPT+^{011} as a function of the two evolution time intervals $\boldsymbol{\tau_1}$ and $\boldsymbol{\tau_2}$. Two protons (two stemming from pH_2) and one carbon at the acetate C1 position were considered (**Fig. S1**). The selective radio frequency pulses were set in resonance with the CHD protons of EP-d$_6$ at the chemical shift of δ = 4.33 ppm. Note that there are 6 evolution intervals in ESOTHERIC (instead of four in phINEPT+) sequence, from which we kept $\boldsymbol{\tau_1} = \boldsymbol{\tau_3}$ as suggested by Korchak and coworkers; also, note that here $\boldsymbol{\tau}$-intervals are half of the $\boldsymbol{\Delta}$-intervals given in the ESOTHERIC scheme in the original work (see our fig. S4).[3] SEPP interval for SEPP-INEPT+ was $\boldsymbol{\tau_0} = \frac{1}{4J_{HH}} \cong$35 ms.

Table S3. Optimal SOT parameters τ_x, total time of SOT t_{total} and simulated polarization P^{th} under this conditions for 1-^{13}C-EP-d$_6$. Note that SEPP-INEPT is 34 ms shorter than the phSPINEPT+^{011} and provides 5 % more polarization. A polarization of ~100% is reached with phSPINEPT+^{011} with a longer sequence (t_{total} = 664 ms).

SOT sequence	$\boldsymbol{\tau_1}$ [ms]	$\boldsymbol{\tau_2}$ [ms]	$\boldsymbol{\tau_0}$ / $\boldsymbol{\tau_3}$ [ms]	$\boldsymbol{t_{total}}$ [ms]	$\boldsymbol{P^{th}}$ [%]
phINEPT+	103	84	-	374	46.2
phSPINEPT+^{011}	103	84	-	374	92
ESOTHERIC	84	36	84	408	100
SEPP-INEPT+	84	72	14	340	97

F. 1-^{13}C- Hydroxyethyl acrylate-d^{8} to 1-^{13}C- Hydroxyethyl propionate-d$_{8}$

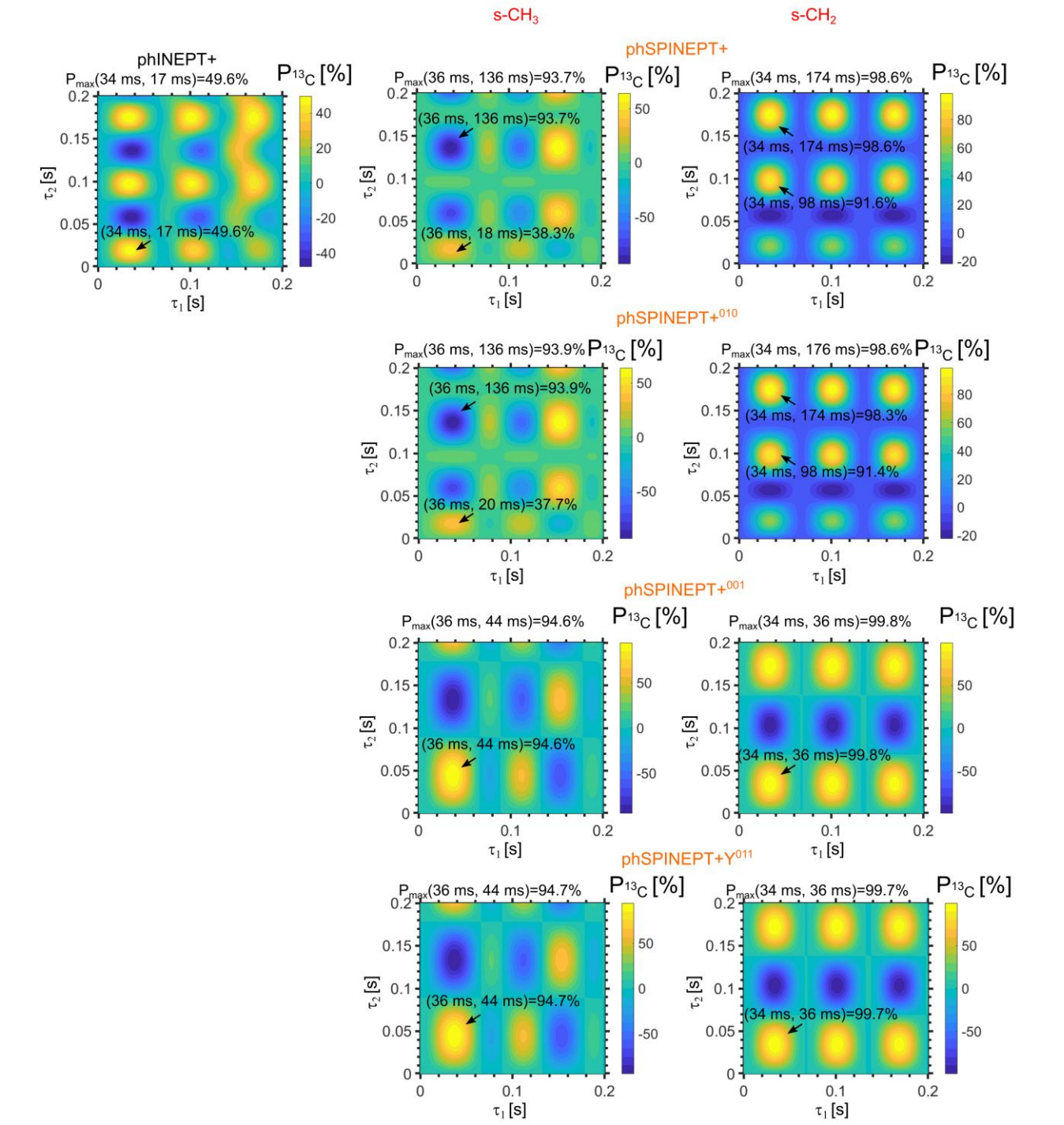

Figure S11. ^{13}C-polarization yield of 1-^{13}C-HEP-d$_{8}$ using phINEPT+ or phSPINEPT+ as a function of the two evolution time intervals τ_1 and τ_2. Two ethyl protons (stemming from pH_2) and one carbon at C1 position were considered (**Fig. S1**). The selective radio frequency pulses were set in resonance with the CH_2 (s-CH_2; at the chemical shift δ = 2.35 ppm) or CH_3 (s-CH_3; at δ = 1.15 ppm) protons of 1-^{13}C-HEP. Note that here complete deuteration of HEA was assumed although experimentally only 1-^{13}C-HEA-d_3 was available (i.e. the $HOCH_2CH_2O$-fragment was not deuterium labeled).

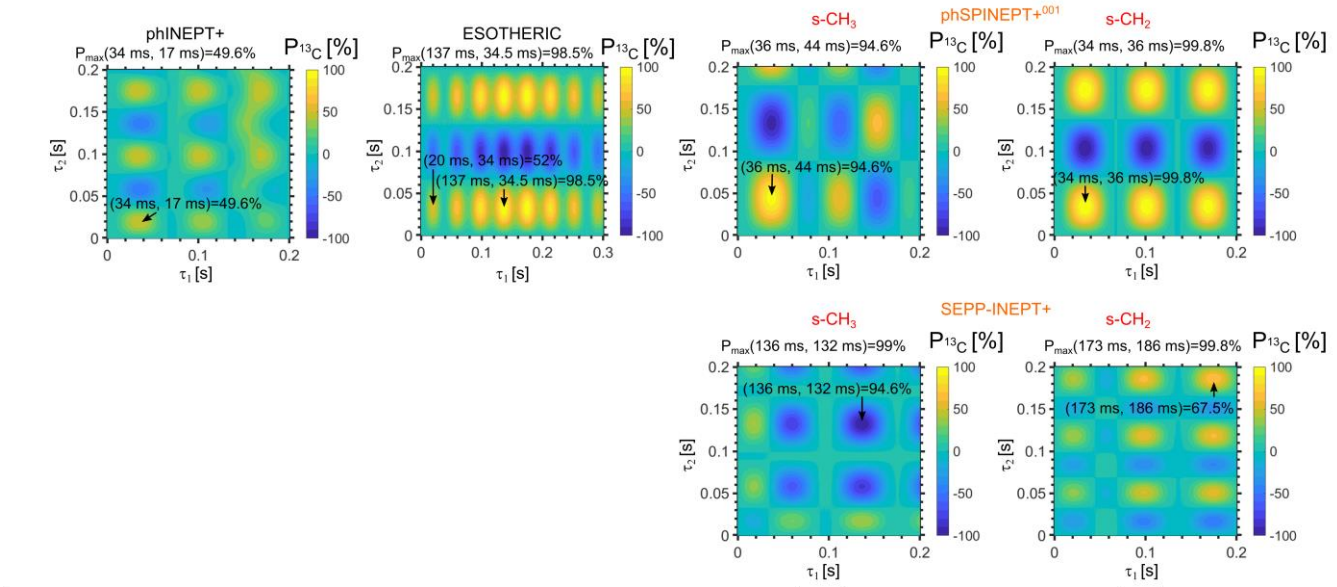

Figure S12. ^{13}C-polarization yield of 1-^{13}C-HEP-d$_8$ phINEPT+, ESOTHERIC,[3] SEPP-INEPT+ and spINEPT+^{011} as a function of the two evolution time intervals $\boldsymbol{\tau_1}$ and $\boldsymbol{\tau_2}$. Two protons (stemming from pH_2) and one carbon at C1 position were considered (Fig. S1). The selective radio frequency pulses were set in resonance with the CH2 (s-CH_2; at the chemical shift δ = 2.35 ppm) or CH_3 (s-CH_3; at δ = 1.15 ppm) protons of 1-^{13}C-HEP. Note that here complete deuteration of HEA was assumed although experimentally only 1-^{13}C-HEA-d3 was available available (i.e. the $HOCH_2CH_2O$- fragment was not deuterium labeled). Note that there are 6 evolution intervals in ESOTHERIC (instead of four in phINEPT+) sequence, from which we kept $\boldsymbol{\tau_1 = \tau_3}$ as suggested by Korchak and coworkers; also, note that here $\boldsymbol{\tau}$-intervals are half of the $\boldsymbol{\Delta}$-intervals given in the ESOTHERIC scheme in the original work (see our Fig. S4).[3] SEPP interval for SEPP-INEPT+ was $\tau_0 = \frac{1}{4J_{HH}} \cong 33$ ms.

Table S4. Optimal SOT parameters τ_x, total time of SOT t_{total} and simulated polarization P^{th} under this conditions for 1-^{13}C-HEP-d$_8$. Note that here ESOTHERIC and SEPP-INEPT+ are much longer than phSPINEPT+^{011}, which provides polarization close to unity. phINEPT+ is shorter but provides only half the polarization. This result and Fig. S14 show that phSPINEPT+^{011} is effective on both, molecules with a "symmetric" and "asymmetric" *J*-coupling pattern.

SOT sequence	$\boldsymbol{\tau_1}$ [ms]	$\boldsymbol{\tau_2}$ [ms]	$\boldsymbol{\tau_0}$ / $\boldsymbol{\tau_3}$ [ms]	$\boldsymbol{t_{total}}$ [ms]	$\boldsymbol{P^{th}}$ [%]
phINEPT+	34	17	-	96	50
phSPINEPT+^{011}	34	36	-	140	99
ESOTHERIC	137	34.5	137	617	99
SEPP-INEPT+	136	132	33	602	95

G. 1-^{13}C- Hydroxyethyl acrylate-d_3 to 1-^{13}C- Hydroxyethyl propionate-d_3

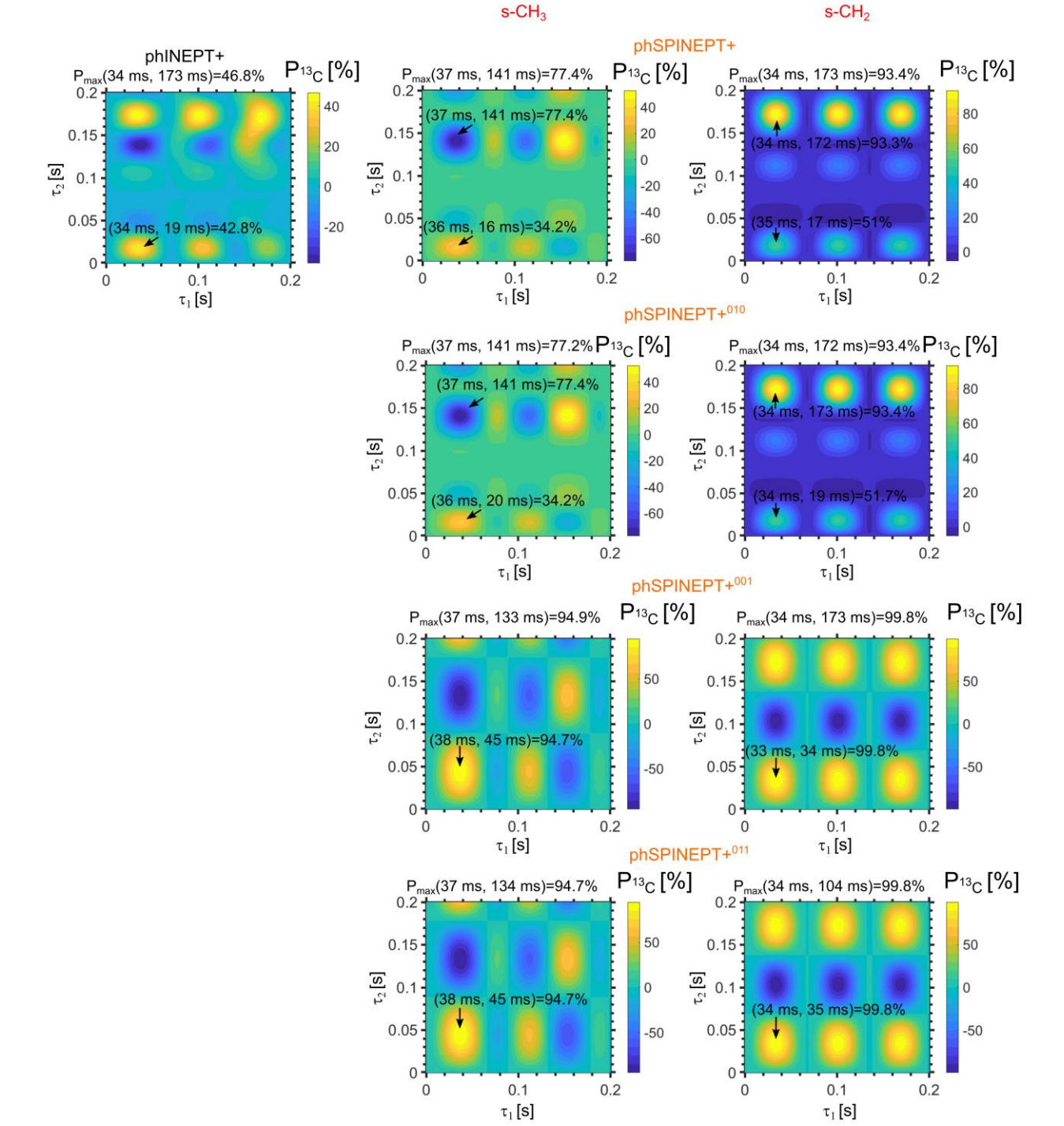

Figure S13. ^{13}C-polarization yield of 1-^{13}C-HEP-d_3 using phINEPT+ or phSPINEPT+ as a function of the two evolution time intervals $\boldsymbol{\tau_1}$ and $\boldsymbol{\tau_2}$. Two ethyl protons (stemming from pH_2), one carbon at C1 position and two other nearest methylene protons were considered (**Fig. S1**). The selective radio frequency pulses were set in resonance with the CH_2 (s-CH_2; at the chemical shift δ = 2.35 ppm) or CH_3 (s-CH_3; at δ = 1.15 ppm) protons of 1-^{13}C-HEP. Note that two other methylene protons were neglected because they do not have observable coupling with C1.

H. Efficiency of phSPINEPT+ in various three spin systems

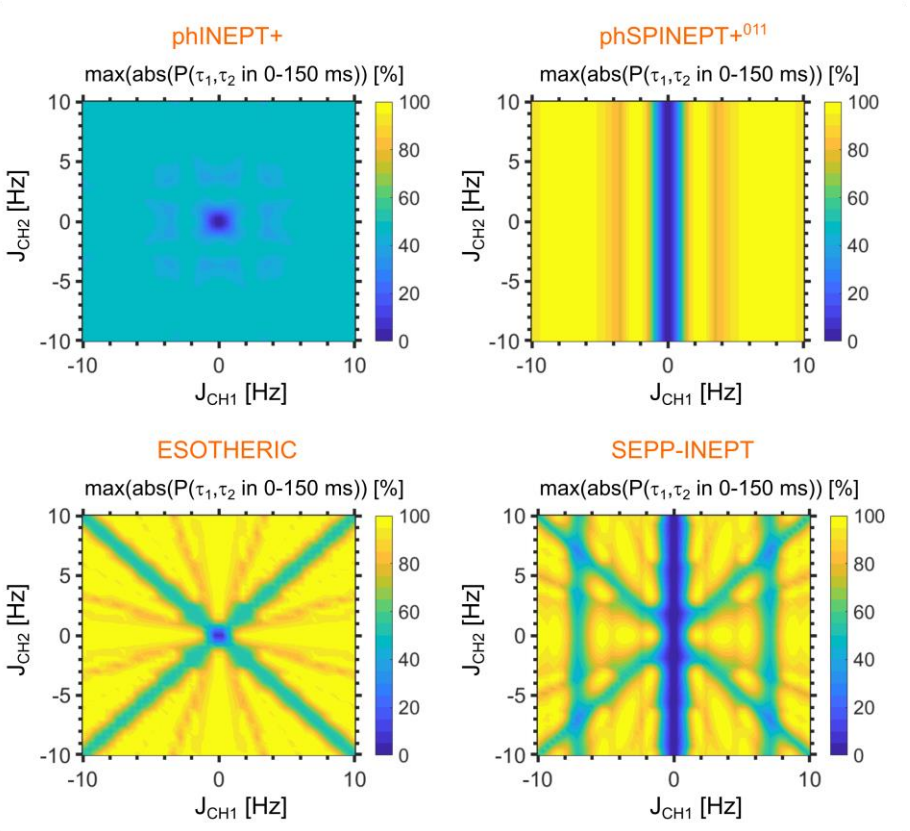

Figure S14. ^{13}C-polarization yield using phSPINEPT+^{011} in arbitrary three spin system as a function of the H-C spin-spin coupling constants. For each pair of J_{CH1} and J_{CH2} the phSPINEPT+^{011} polarization was calculated as a function of the evolution timings $\boldsymbol{\tau_1}$ and $\boldsymbol{\tau_2}$. From this data, the absolute maximum of the polarization was extracted and is displayed in this figure. $\boldsymbol{\tau_1}$ and $\boldsymbol{\tau_2}$ intervals were varied in the range of 0 to 150 ms in steps of 2 ms. Proton chemical shift difference was 3 ppm, their mutual spin-spin coupling, J_{H1H2}, was fixed at 7 Hz, magnetic field was set to $\boldsymbol{B_0}$ = 9.4 T. The selective pulses were applied on the H1 nucleus.

4.3. phINEPT+ and phSPINEPT+ spectra (Experimental)

A. 1-^{13}C-Vinyl acetate to 1-^{13}C-ethyl acetate

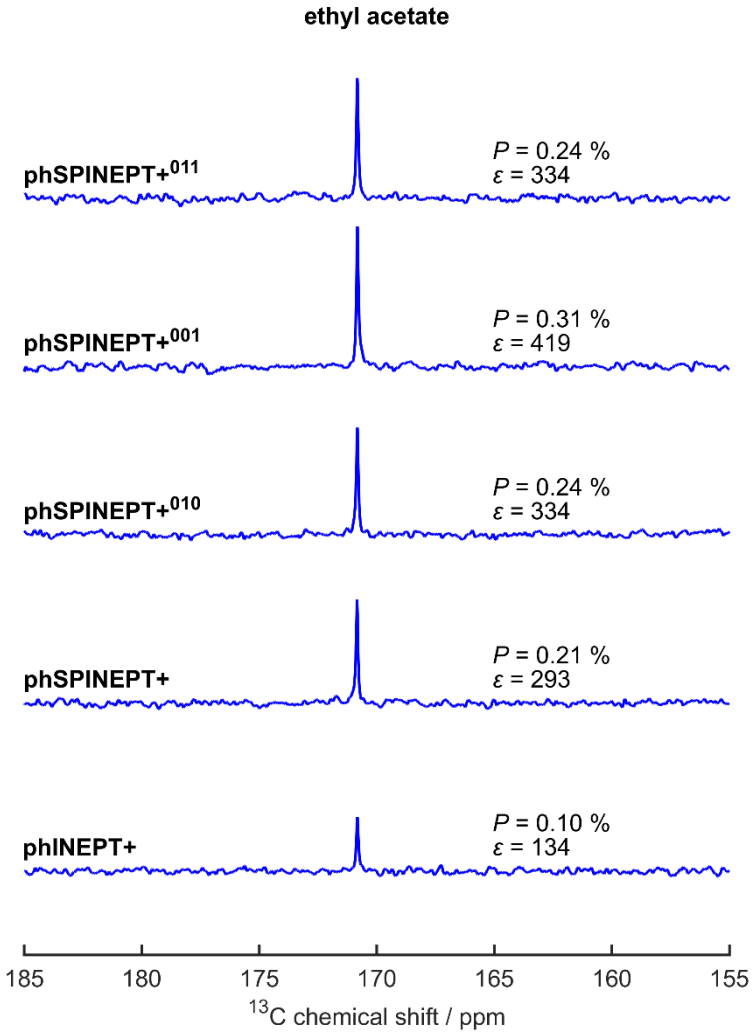

Figure S15. ^{13}C-NMR spectra of 1-^{13}C-hyperpolarized ethyl acetate using the phINEPT+ and phSPINEPT+ SOT sequences. The used experimental parameters are summarized in **Tab S1**.

B. 1-^{13}C-Vinyl acetate-d_6 to 1-^{13}C-ethyl acetate-d_6

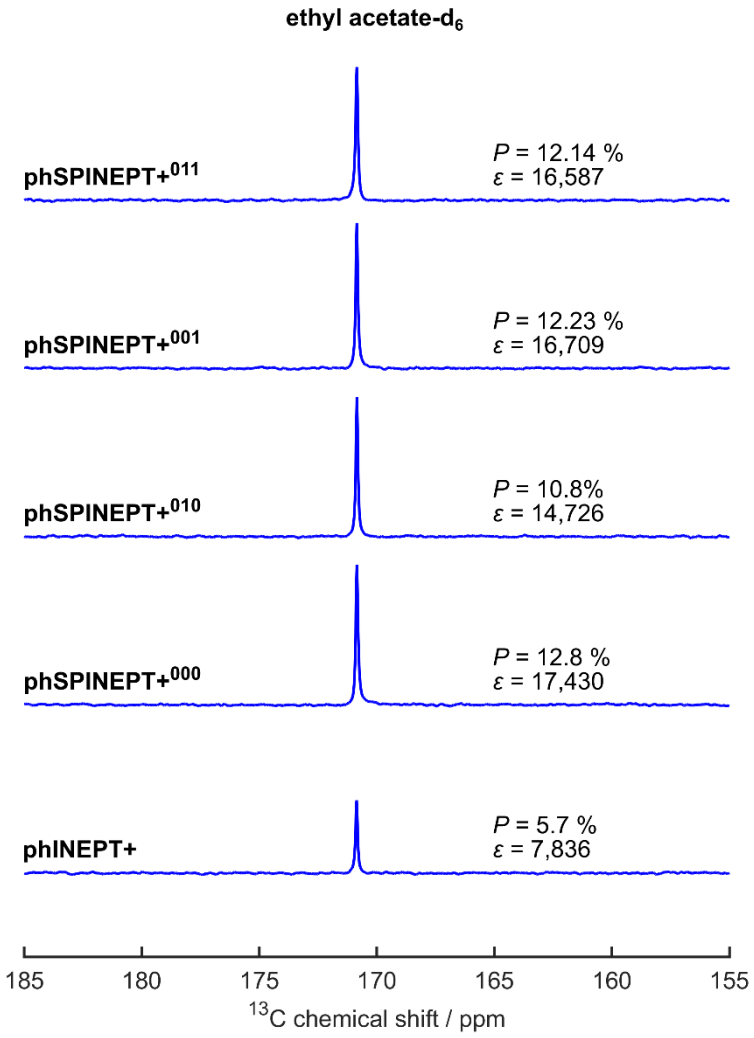

Figure S16. ^{13}C-NMR spectra of 1-^{13}C-hyperpolarized ethyl acetate-d_6 using the phINEPT+ and phSPINEPT+ SOT sequences. The used experimental parameters are summarized in **Tab S1**.

C. 1-^{13}C-Vinyl pyruvate to 1-^{13}C-ethyl pyruvate

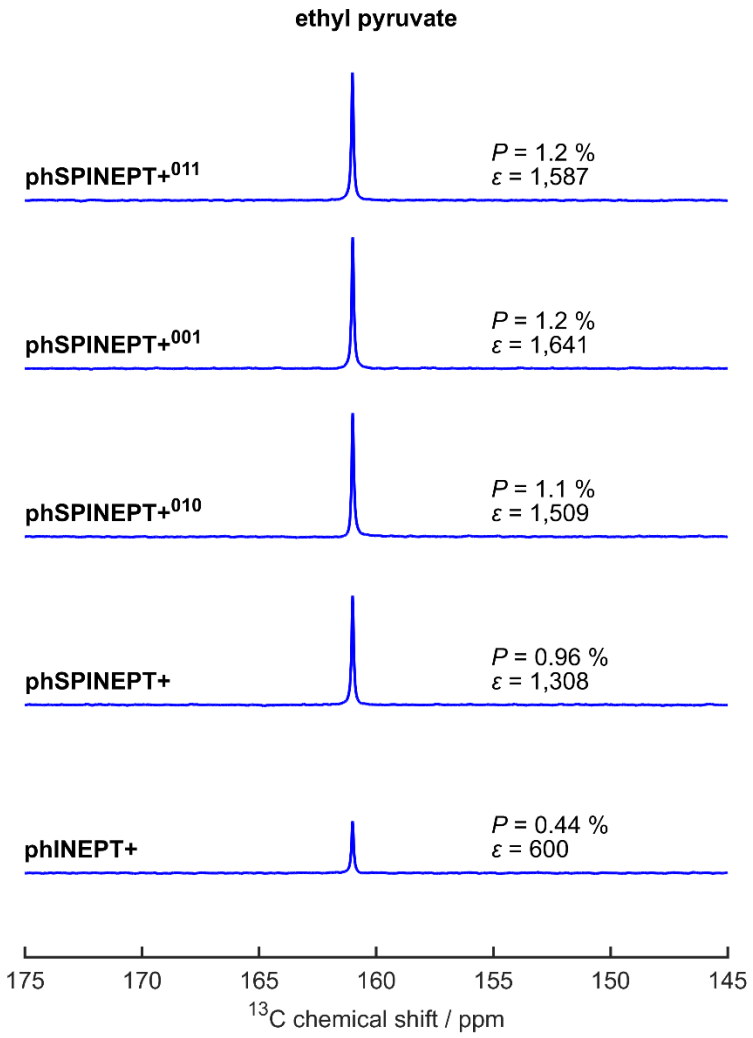

Figure S17 ^{13}C-NMR spectra of 1-^{13}C-hyperpolarized ethyl pyruvate using the phINEPT+ and phSPINEPT+ SOT sequences. The used experimental parameters are summarized in **Tab S1**.

D. 1-^{13}C-hydroxyethyl acrylate-d_3 to 1-^{13}C-hydroxyethyl propionate-d_3

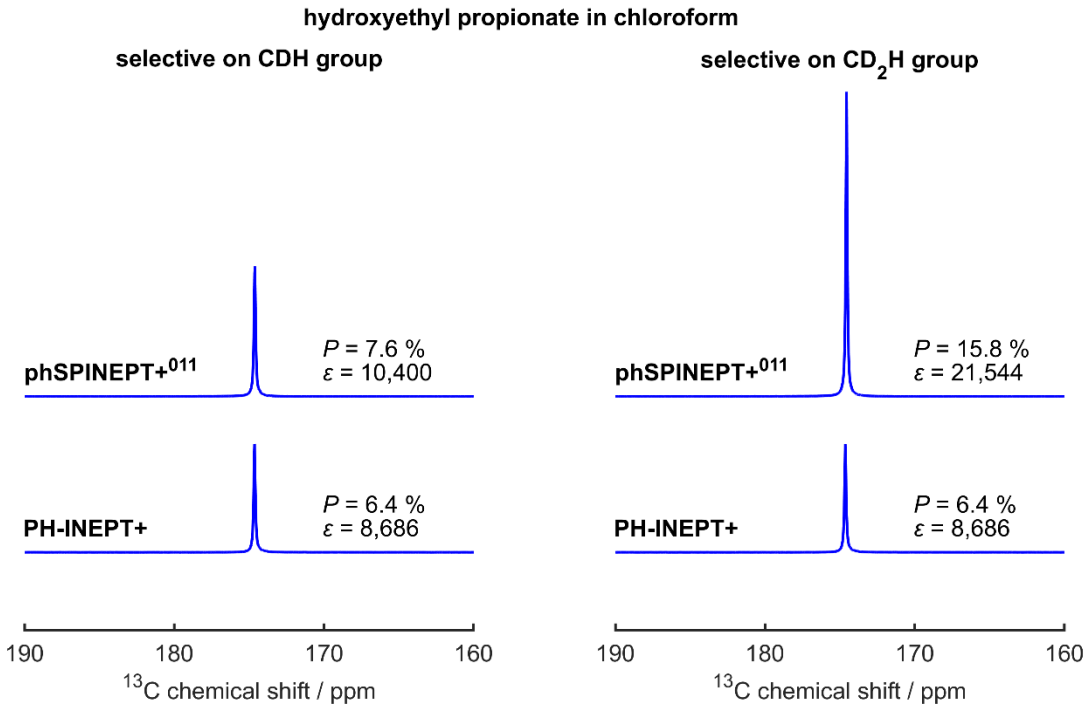

Figure S18. ^{13}C-NMR spectra of 1-^{13}C-hyperpolarized hydroxyethyl propionate-d_3 in chloroform-d using the phINEPT+ and phSPINEPT+ SOT sequences. The used experimental parameters are summarized in **Tab S1**.

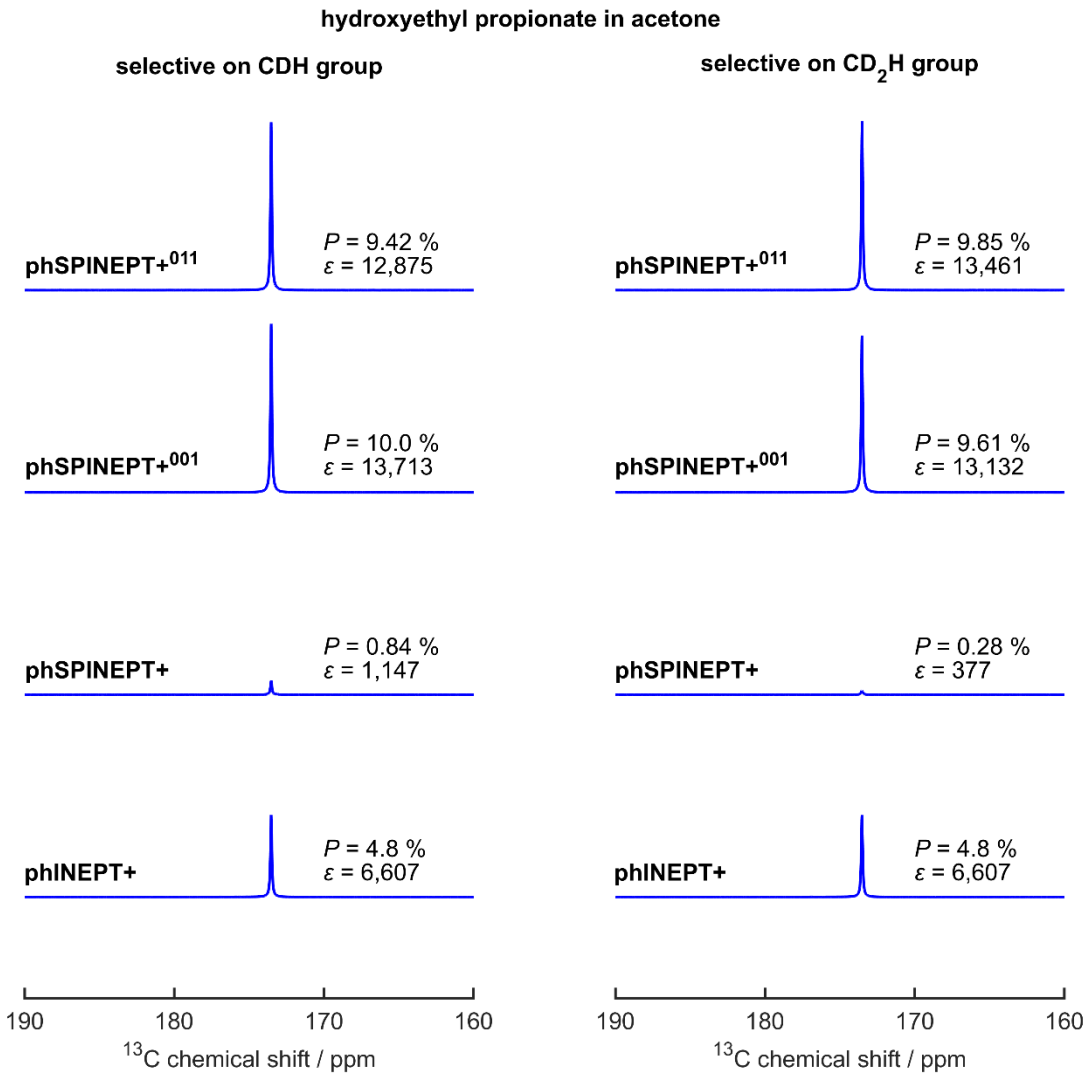

Figure S19. ^{13}C-NMR spectra of 1-^{13}C-hyperpolarized hydroxyethyl propionate-d$_3$ in acetone-d$_6$ using the phINEPT+ and phSPINEPT+ SOT sequences. Not all experimentally used parameters were identical to the one that according to our simulations give optimal polarization. The used experimental parameters are summarized in **Tab S1** and correpsonding polarization maps are presented in **Fig S12**.

5. **Estimation of hydrogenation reaction and magnetization decay**

We consider a reaction of substrate *A* to product *B* which creates magnetization M_B that subsequently relaxes to 0 with rate *R*:

$A \xrightarrow{k_{hyd}} B$ [eq S1]

$M_B \xrightarrow{R} 0$ [eq S2]

The concentration of product at a time t is

$[B](t) = [A_0]\left(1 - e^{-tk_{hyd}}\right)$ [eq S3]

The change of concentration of product B in the interval (t,t+dt) is

$d[B](t) = [A_0]k_{hyd}e^{-tk_{hyd}}dt$ [eq S4]

Then magnetization (without nuclear dipol moment for simplicity or in the units of polarization times concentration) that is generated in the same time interval is given by

$dM_B(t,t) = P_{max}d[B](t) = [A_0]k_{hyd}e^{-tk_{hyd}}dt$ [eq S5]

The remaining magnetization at time point τ which was generated in the interval (t,t+dt) is

$dM_B(t,\tau) = [A_0]P_{max}k_{hyd}e^{-R(\tau-t)}e^{-tk_{hyd}}dt$ [eq S6]

The total magnetization at time point τ then can be calculated by a simple integration over t:

$$M_B(\tau) = P(\tau)[B](\tau) = \int_0^\tau dM_B(t,\tau)dt = [A_0]P_{max}k_{hyd}e^{-R\tau}\int_0^\tau e^{-t\left(k_{hyd}-R\right)}dt =$$

$= [A_0]P_{max}\frac{1}{1-R/k_{hyd}}\left(e^{-R\tau} - e^{-\tau k_{hyd}}\right)$ [eq S7]

And in terms of remaining polarization that is usually reported in the literature

$P(\tau) = P_{max}\frac{1}{1-\frac{R}{k_{hyd}}}\frac{e^{-R\tau}-e^{-\tau k_{hyd}}}{1-e^{-\tau k_{hyd}}}$ [eq S8]

If we assume that $R \ll k_{hyd}$, which is justified because $R \sim \frac{1}{T_1} < 0.25\ \mathrm{s}^{-1}$ for all measured T_1 values (Fig. S.1) and in ≈6 seconds we achieved complete hydrogenation (i.e. $k_{\mathrm{hyd}} \geq \frac{5}{6}\mathrm{s}^{-1} \approx 0.8\ \mathrm{s}^{-1}$), then

$[B]\left(\tau \gg 1/k_{hyd}\right) \cong [A_0]$ [eq S9]

And

$M_B\left(\frac{1}{R} \gg \tau \gg \frac{1}{k_{hyd}}\right) = P(\tau)[B](\tau) \cong [A_0]P_{max}e^{-R\tau}$ [eq S10]

Then polarization is

$P(\tau) \cong P_{max}e^{-R\tau}$ [eq S11]

Under the assumption of a very fast hydrogenation compared to relaxation equations eq S7 and S8 simplify to eq S10 and S11 respectively. Eq S11 was used in the main manuscript.

To make sure that in the model no division by zero happens, let us also consider the case when $k_{hyd} = R + \Delta$ with $\Delta \ll R, k_{hyd}$, i.e. when $k_{hyd} \cong R$.

Then simplification of eq S7 results in

$$M_B(\tau, k_{hyd} \cong R) = [A_0]P_{max}\frac{e^{-R\tau}}{1-\frac{1}{1+\frac{\Delta}{R}}}(1 - e^{-\tau\Delta}) = [A_0]P_{max}\frac{e^{-R\tau}}{1-1+\frac{\Delta}{R}}(1 - 1 + \tau\Delta) =$$

$$= [A_0]P_{max}\tau R e^{-R\tau} \quad \text{[eq S12]}$$

The $M_B(\tau, k_{hyd} \cong R)$ reaches its maximum of $[A_0]P_{max}e^{-1}$ when $\tau = 1/R$.

Under the same conditions eq S8 gives

$$P(\tau, k_{hyd} \cong R) = P_{max}\frac{e^{-R\tau}}{1-\frac{1}{1+\Delta/R}}\frac{1-e^{-\tau\Delta}}{1-e^{-\tau R}} = P_{max}\frac{e^{-R\tau}}{1-1+\frac{\Delta}{R}}\frac{1-1+\tau\Delta}{1-e^{-\tau R}} = P_{max}\frac{R\tau}{e^{R\tau}-1} \text{ [eq S13].}$$

The function reaches maximum (for positive τ) at $\tau = 0$. Hence to maximise polarization this conditions must be avoided and k_{hyd} should be much faster than R.

6. Scripts: pulse sequences (Bruker code)

Below, the general SOT scheme with ^{1}H decoupling is given, and all variants of used SOTs.

A. SOT frame

```
#include <Avance.incl>
"acqt0=-p1*2/3.1416"
"p11=p1/2" ; 13C:45
"p12=p1*2" ; 13C:180
"p21=p2/2" ; 1H: 45
"p22=p2*2" ; 1H: 180
1 ze
2 30m do:f2
        d1
        10m LOCKH_ON
        30m pl1:f1
        30m pl2:f2
        ; put your pH2 bubbling script here
        ; <SOT script>
        go=2 ph31
        30m LOCKH_OFF do:f2 mc #0 to 2 F0(zd)
exit
ph1=0
ph2=1
ph31=0
```

B. SOT: phINEPT+

```
(p21 ph2):f2
        d5 ; d5 = tau1/2
(center (p12 ph1):f1 (p22 ph1):f2)
        d5 ; d5 = tau1/2
(center (p1 ph1):f1  (p2 ph2):f2)
        d6 ; d6 = tau2/2
        1u
(center (p12 ph1):f1            (p22 ph1):f2)
        d6 pl12:f2 ; d6 = tau2/2
1u cpd2:f2
```

C. SOT: phSPINEPT+

```
(p10:sp1 ph2):f3
        d4 pl2:f3 ; d4 = tau1/2-p10/2
(center (p12 ph1):f1 (p22 ph1):f3)
        d5 ; d5 = tau1/2
(center (p1 ph1):f1  (p2 ph2):f3)
        d6 ; d6 = tau2/2
        1u
(center (p12 ph1):f1 (p22 ph1):f3)
        d6 pl12:f2 ; d6 = tau2/2
1u cpd2:f2
```

D. SOT: phSPINEPT+^{001}

```
(p10:sp1 ph2):f3
        d4 pl2:f3 ; d4 = tau1/2-p10/2
(center (p12 ph1):f1 (p22 ph1):f3)
        d5 ; d5 = tau1/2
(center (p1 ph1):f1 (p2 ph2):f3)
        d6 ; d6 = tau2/2-p10/2
        1u
(center (p12 ph1):f1 (p10:sp2 ph1):f3)
        d7 pl12:f2 ; d7 = tau2/2-p10/2
1u cpd2:f2
```

E. phSPINEPT+^{010}

```
(p10:sp1 ph2):f3
        d4 pl2:f3 ; d4 = tau1/2-p10/2
(center (p12 ph1):f1 (p22 ph1):f3)
        d5 ; d5 = tau1/2-p10/2
(center (p1 ph1):f1 (p10:sp1 ph2):f3)
        d6 pl2:f3 ; d6 = tau2/2-p10/2
        1u
```

```
(center (p12 ph1):f1 (p22 ph1):f3)
        d7 pl12:f2 ; d7 = tau2/2
1u cpd2:f2
```

F. phSPINEPT+[011]

```
(p10:sp1 ph2):f3
        d4 pl2:f3 ; d4 = tau1/2-p10/2
(center (p12 ph1):f1 (p22 ph1):f3)
        d5 ; d5 = tau1/2-p10/2
(center (p1 ph1):f1 (p10:sp1 ph2):f3)
        d6 ; d6 = tau2/2-p10
        1u
(center (p12 ph1):f1 (p10:sp2 ph1):f3)
        d7 pl12:f2 ; d7 = tau2/2
1u cpd2:f2
```

7. References

(1) Schmidt, A. Liquid-State Nuclear Hyperpolarization without a Polarizer : Synthesis amid the Magnet Bore Allows a Dramatically Enhanced Nuclear Alignment. **2020**. https://doi.org/10.6094/UNIFR/165763.

(2) Barkemeyer, J.; Bargon, J.; Sengstschmid, H.; Freeman, R. Heteronuclear Polarization Transfer Using Selective Pulses during Hydrogenation with Parahydrogen. *Journal of Magnetic Resonance, Series A* **1996**, *120* (1), 129–132. https://doi.org/10.1006/jmra.1996.0109.

(3) Korchak, S.; Mamone, S.; Glöggler, S. Over 50 % 1H and 13C Polarization for Generating Hyperpolarized Metabolites—A Para-Hydrogen Approach. *ChemistryOpen* **2018**, *7* (9), 672–676. https://doi.org/10.1002/open.201800086.

(4) Hövener, J.-B.; Bär, S.; Leupold, J.; Jenne, K.; Leibfritz, D.; Hennig, J.; Duckett, S. B.; von Elverfeldt, D. A Continuous-Flow, High-Throughput, High-Pressure Parahydrogen Converter for Hyperpolarization in a Clinical Setting. *NMR Biomed.* **2013**, *26* (2), 124–131. https://doi.org/10.1002/nbm.2827.

(5) Pravdivtsev, A. N.; Hövener, J.-B. Simulating Non-Linear Chemical and Physical (CAP) Dynamics of Signal Amplification By Reversible Exchange (SABRE). *Chem. Eur. J.* **2019**, *25* (32), 7659–7668. https://doi.org/10.1002/chem.201806133.